symmetry

MDPI

*Article*

# Fractals as Julia and Mandelbrot Sets of Complex Cosine Functions via Fixed Point Iterations

**Anita Tomar [1], Vipul Kumar [2], Udhamvir Singh Rana [2] and Mohammad Sajid [3,*]**

1 Pt. Lalit Mohan Sharma Campus, Sridev Suman Uttarakhand University, Rishikesh 249201, Uttarakhand, India
2 D.A.V. College, Dehradun 248001, Uttarakhand, India
3 Department of Mechanical Engineering, College of Engineering, Qassim University, Buraydah 51452, Saudi Arabia
* Correspondence: msajd@qu.edu.sa; Tel.: +966-16-30-13761

**Abstract:** In this manuscript, we explore stunning fractals as Julia and Mandelbrot sets of complex-valued cosine functions by establishing the escape radii via a four-step iteration scheme extended with s-convexity. We furnish some illustrations to determine the alteration in generated graphical images and study the consequences of underlying parameters on the variation of dynamics, colour, time of generation, and shape of generated fractals. The black points in the obtained fractals are the "non-chaotic" points and the dynamical behaviour in the black area is easily predictable. The coloured points are the points that "escape", that is, they tend to infinity under one of iterative methods based on a four-step fixed-point iteration scheme extended with s-convexity. The different colours tell us how quickly a point escapes. The order of escaping of coloured points is red, orange, yellow, green, blue, and violet, that is, the red point is the fastest to escape while the violet point is the slowest to escape. Mostly, these generated fractals have symmetry. The Julia set, where we find all of the chaotic behaviour for the dynamical system, marks the boundary between these two categories of behaviour points. The Mandelbrot set, which was originally observed in 1980 by Benoit Mandelbrot and is particularly important in dynamics, is the collection of all feasible Julia sets. It perfectly sums up the Julia sets.

**Keywords:** chaotic behaviour; convexity; escape criterion; escape radii; four-step fixed-point iteration; iterative methods; fractals; Julia set; Mandelbrot set; symmetry

**MSC:** 70K55; 39B62; 28A10; 39B12; 47H10; 37F10; 37F45

check for updates

**Citation:** Tomar, A.; Kumar, V.; Rana, U.S.; Sajid, M. Fractals as Julia and Mandelbrot Sets of Complex Cosine Functions via Fixed Point Iterations. *Symmetry* **2023**, *15*, 478. https://doi.org/10.3390/sym15020478

Academic Editor: Alexander Zaslavski

Received: 8 January 2023
Revised: 24 January 2023
Accepted: 30 January 2023
Published: 10 February 2023



## 1. Introduction and Preliminaries

The fixed-point theory is a significant branch of mathematics since fixed-point conclusions are useful in solving numerous real-life mathematical problems which can be expressed as functional equations. One of the most crucial challenges in iterative methods is that of developing useful fixed-point iterations to speed up the approximation or calculation of the fixed point of underlying problems. Some researchers developed distinct iteration schemes to overcome this issue. For instance, Abbas et al. [1], Agarwal et al. [2], Alfuraidan and Khamsi [3], Berinde [4], Ishikawa [5], Mann [6], Noor [7], Picard [8], Sintunavarat and Pitea [9], etc. The theory of fixed points via distinct fixed-point iteration schemes or iterative methods may be applied to obtain stunning fractals which find applications in numerous nonlinear phenomena appearing in various branches of science. For example, computer science [10], biotechnology [11], engineering [12], biology [13], physics [14], and so on. The Julia set is the place where all of the chaotic behaviour of the complex-valued function occurs. The collection of all possible Julia sets of an underlying function is the Mandelbrot set which helps us in understanding the totality of all Julia set shapes. Recently, fractal geometry has been widened to encompass a variety of unique roles, such as higher-degree polynomials, exponential, rational, and trigonometric functions, etc., using existing fixed-point iteration schemes or iterative methods (as can be seen in Abbas et al. [15], Husain et al. [16], Kumar et al. [17], Prajapati et al. [18], Shahid et al. [19], Tanveer et al. [20], Tomar et al. [21], etc.).

The present work, inspired by Antal et al. [22] and Ozgur et al. [23], studied Julia and Mandelbrot sets of complex cosine functions using a four-step iteration scheme extended by s-convexity to develop the escape criterion. We first extend the existing four-step iteration scheme [24] with s-convexity to develop the escape criterion and then furnish some graphical examples using the proven escape criteria, developed an escape time algorithm, colour map, and MATLAB software. The developed escape time algorithm is focused on the minimum number of iterations that are essential to decide whether the sequence orbit tends to infinity. It is well known that the escape threshold is different for different functions as well as different iterations and has a substantial impact on the exploration of fractals. It is observed that most generated fractals have symmetry. We give concluding remarks to compare the effectiveness and efficiency of our iteration scheme or iterative method in the generation of fractals with the existing work in the literature. Furthermore, we discuss the variation in structure, colour, area, and the time taken to explore the Julia and Mandelbrot sets when we change the parameters involved in the underlying cosine functions as well as in the four-step iteration endowed with s-convexity. The colours of the explored Julia sets depend on both the number of iterations as well as the values of input parameters. Furthermore, the conclusions of this work unlock new avenues of transcendental complex-valued functions for fractals as Julia and Mandelbrot sets; and may be used for other iterative methods.

**Definition 1.** *(Julia set [10,25]) The collection of points in a set of complex numbers so that the orbit to the function $T : \mathbb{C} \to \mathbb{C}$, diverging to the point at infinity, is called the filled Julia set of $T$. We denote it by $S_T$ and write*

$$S_T = \{z \in \mathbb{C} : \{|T^i(z)|\}_{i=0}^{\infty} \text{ is bounded}\}.$$

The Julia set of $T$ is the boundary of $S_T$.

**Definition 2.** *(Mandelbrot set [26,27]) The collection of parameters $c$ in a set of complex numbers so that the filled Julia set $S_T$ of $T = z^2 + c$ is connected and called the Mandelbrot set, that is,*

$$M = \{c \in \mathbb{C} : S_T \text{ is connected}\}.$$

*In other words, $M$ contains enormous facts related to the Julia sets and is also described as*

$$M = \{c \in \mathbb{C} : |T(z)| \nrightarrow \infty \text{ as } k \to \infty\}.$$

**Definition 3.** *(Four-step iteration [24]) Consider the sequence $\{z_k\}$ of iterates for the initial point $z_0 \in \mathbb{C}$ and $T : \mathbb{C} \to \mathbb{C}$ to be a complex-valued self-mapping. The four-step iteration scheme for the sequence $\{z_k\}$ is defined as*

$$\begin{aligned} w_k &= (1-\delta)z_k + \delta T z_k, \\ x_k &= (1-\gamma)z_k + \gamma T w_k, \\ y_k &= (1-\beta)z_k + \beta T x_k, \\ z_{k+1} &= (1-\alpha)z_k + \alpha T y_k, \end{aligned}$$

*where $k \in \mathbb{N} \cup \{0\}$ and $\alpha, \beta, \gamma, \delta \in (0, 1]$.*

Notice that it is a four-step procedure. The above sequence of iterates $\{z_n\}$ can be reduced to the Picard orbit, Mann orbit, Ishikawa orbit, and Noor orbit, where the first two are one-step procedures, the third is a two-step procedure and the last is a three-step procedure.

1. The Picard orbit [8] when $\beta, \gamma, \delta = 0$ and $\alpha = 1$.
2. The Mann orbit [6] when $\beta, \gamma, \delta = 0$.
3. The Ishikawa orbit [5] when $\gamma, \delta = 0$.
4. The Noor orbit [7] when $\delta = 0$.

**Definition 4.** *(s-convex combination [28]) Let $z_1, z_2, \ldots, z_n \in \mathbb{C}$ and $s \in (0,1]$. The s-convex combination is described as*

$$\lambda_1^s.z_1 + \lambda_2^s.z_2 + \lambda_3^s.z_3 + \ldots + \lambda_n^s.z_n, \tag{1}$$

*where $\lambda_k \geq 0$ and $\sum_{k=1}^{n} \lambda_k = 1$ for $k \in 1, 2, \ldots, n$.*

For s = 1, the s-convex combination diminishes to the standard convex combination. Now, we endow the four-step iteration with the s-convex combination and write,

$$\begin{aligned} w_k &= (1-\delta)^s z_k + \delta^s T z_k, \\ x_k &= (1-\gamma)^s z_k + \gamma^s T w_k, \\ y_k &= (1-\beta)^s z_k + \beta^s T x_k, \\ z_{k+1} &= (1-\alpha)^s z_k + \alpha^s T y_k. \end{aligned}$$

This is called a four-step iteration extended with s-convexity.

## 2. Escape Criteria for Complex Cosine Functions

The escape criterion performs an essential role in generating and analysing Julia sets as well as Mandelbrot sets and their variants. We develop the following escape criteria for the complex-valued cosine functions to explore and compare the new mutants of Julia and Mandelbrot sets via our four-step iteration scheme extended with s-convexity.

**Theorem 1.** *Let $T(z) = \cos(z^k) + az + c$; $k \geq 2$; $|z| \geq |c| > (\frac{2+|a|}{s\alpha|\omega_1|})^{\frac{1}{k-1}}$, $|z| \geq |c| > (\frac{2+|a|}{s\beta|\omega_2|})^{\frac{1}{k-1}}$, $|z| \geq |c| > (\frac{2+|a|}{s\gamma|\omega_3|})^{\frac{1}{k-1}}$, and $|z| \geq |c| > (\frac{2+|a|}{s\delta|\omega_4|})^{\frac{1}{k-1}}$, $a, c \in \mathbb{C}$. If the sequence $\{z_k\}$ is a four-step iteration scheme extended with s-convexity, then $|z_k| \to \infty$ as $k \to \infty$.*

**Proof.** Suppose $T(z) = \cos(z^k) + az + c$, and

$$|w_k| = |(1-\delta)^s z_k + \delta^s T(z_k)|.$$

If $k = 0$ and $z_0 = z$,

$$\begin{aligned} |w_0| &= |(1-\delta)^s z + \delta^s T(z)| \\ &= |(1-\delta)^s z + \delta^s(\cos(z^k) + az + c)| \\ &\geq |(1-\delta)^s z + s\delta(\cos(z^k) + az + c)|, \ (since \ \ \delta, s \in (0,1], \ \ so \ \ \delta^s \geq s\delta) \\ &\geq |s\delta(\cos(z^k) + az) + (1-\delta)^s z| - s\delta|c| \\ &\geq |s\delta(\cos(z^k) + az) + (1-\delta)^s z| - s\delta|z|, \ \ (since \ |z| \geq |c|), \\ &\geq |s\delta(\cos(z^k) + az)| - |(1-\delta)^s z| - s\delta|z|. \end{aligned}$$

Expanding $(1-\delta)^s$ utilizing binomial theorem up to linear terms of $\delta$, we obtain

$$\begin{aligned}|w_0| &\geq |s\delta(\cos(z^k)+az)| - |(1-s\delta)z| - s\delta|z| \\ &\geq |s\delta(\cos(z^k)+az)| - |z| + |s\delta z| - s\delta|z| \\ &\geq s\delta|\cos(z^k)| - s\delta|a||z| - |z| \\ &\geq s\delta|\cos(z^k)| - |a||z| - |z|, \;\; s,\delta \in (0,1].\end{aligned}$$

Since it is well known that $|\cos(z^k)| \leq 1, \forall\, z \in \mathbb{C}$,

$$|\cos(z^k)| = |1 - \frac{z^{2k}}{2!} + \frac{z^{4k}}{4!} - \dots| \geq |\omega_4|.|z^k|,$$

where $|\omega_4| \in (0,1]$ except the value of $z$ for which $|\omega_4| = 0$.

$$\begin{aligned}|w_0| &\geq s\delta|\omega_4|.|z^k| - |z|(1+|a|) \\ &\geq |z|[s\delta|\omega_4|.|z^{k-1}| - (1+|a|)].\end{aligned}$$

Since

$$|z| > (\frac{2+|a|}{s\delta|\omega_4|})^{\frac{1}{k-1}},$$

implies that,

$$|w_0| \geq |z|. \tag{2}$$

Now, for the next step of the four-step iteration, we obtain

$$|x_k| = |(1-\gamma)^s z_k + \gamma^s T(w_k)|.$$

Again, if $k=0$, $z_0 = z$, and $w_0 = w$,

$$\begin{aligned}|x_0| &= |(1-\gamma)^s z + \gamma^s T(w)| \\ &= |(1-\gamma)^s z + \gamma^s(\cos(w^k)+aw+c)|, \;\; (\gamma, s \in (0,1],\ so\ \ \gamma^s \geq s\gamma) \\ &\geq |(1-\gamma)^s z + s\gamma(\cos(w^k)+aw+c)| \\ &\geq |s\gamma(\cos(w^k)+aw) + (1-\gamma)^s z| - s\gamma|c| \\ &\geq |s\gamma(\cos(w^k)+aw) + (1-\gamma)^s z| - s\gamma|z|, \;\; (since\ |z| \geq |c|), \\ &\geq |s\gamma(\cos(w^k)+aw)| - |(1-\gamma)^s z| - s\gamma|z|.\end{aligned}$$

Expanding $(1-\gamma)^s$ utilizing the binomial theorem up to linear terms of $\gamma$, we obtain

$$\begin{aligned}|x_0| &\geq |s\gamma(\cos(w^k)+aw)| - |(1-s\gamma)z| - s\gamma|z| \\ &\geq |s\gamma(\cos(w^k)+aw)| - |z| + |s\gamma z| - s\gamma|z| \\ &\geq s\gamma|\cos(w^k)| - s\gamma|a||w| - |z| \\ &\geq s\gamma|\cos(w^k)| - |a||w| - |z|, \;\; (s,\gamma \in (0,1]).\end{aligned}$$

Since it is well known that $|\cos(w^k)| \leq 1, \forall\, w \in \mathbb{C}$, then

$$|\cos(w^k)| = |1 - \frac{w^{2k}}{2!} + \frac{w^{4k}}{4!} - \dots| \geq |\omega_3||w^k|,$$

where $|\omega_3| \in (0,1]$ except the value of $w$ for which $|\omega_3| = 0$.

$$|x_0| \geq s\gamma|\omega_3||w^k| - |a||w| - |z|.$$

Using Equation (2), we obtain

$$\begin{aligned}|x_0| &\geq s\gamma|\omega_3||z^k| - |z||a| - |z|, \quad (s, \gamma, \in (0,1]) \\ &\geq |z|[s\gamma|\omega_3||z^{k-1}| - (1 + |a|)].\end{aligned}$$

Since

$$|z| > (\frac{2 + |a|}{s\gamma|\omega_3|})^{\frac{1}{k-1}}$$

implies that

$$|x_0| \geq |z|. \tag{3}$$

Now, for the next step of the four-step iteration, we obtain

$$|y_k| = |(1-\beta)^s z_k + \beta^s T(x_k)|.$$

Again, if $k = 0$, $z_0 = z$, and $x_0 = x$,

$$\begin{aligned}|y_0| &= |(1-\beta)^s z + \beta^s T(x)| \\ &= |(1-\beta)^s z + \beta^s(\cos(x^k) + ax + c)| \ (\ since \ \ \beta, s \in (0,1], \ so \ \ \beta^s \geq s\beta) \\ &\geq |(1-\beta)^s z + s\beta(\cos(x^k) + ax + c)| \\ &\geq |s\beta(\cos(x^k) + ax) + (1-\beta)^s z| - s\beta|c|\end{aligned}$$

$$\begin{aligned}&\geq |s\beta(\cos(x^k) + ax) + (1-\beta)^s z| - s\beta|z|, \quad (|z| \geq |c|) \\ &\geq |s\beta(\cos(x^k) + ax)| - |(1-\beta)^s z| - s\beta|z|.\end{aligned}$$

Expanding $(1-\beta)^s$ utilizing binomial theorem up to linear terms of $\beta$, we attain

$$\begin{aligned}|y_0| &\geq |s\beta(\cos(x^k) + ax)| - |(1 - s\beta)z| - s\beta|z| \\ &\geq |s\beta(\cos(x^k) + ax)| - |z| + s\beta|z| - s\beta|z| \\ &\geq s\beta|\cos(x^k)| - s\beta|a||x| - |z| \\ &\geq s\beta|\cos(x^k)| - |a||x| - |z|, \quad s, \beta \in (0,1].\end{aligned}$$

Since it is well known that $|\cos(x^k)| \leq 1, \forall\ x \in \mathbb{C}$, then

$$|\cos(x^k)| = |1 - \frac{x^{2k}}{2!} + \frac{x^{4k}}{4!} - \ldots| \geq |\omega_2|.|x^k|,$$

where $|\omega_2| \in (0,1]$ except the value of $x$ for which $|\omega_2| = 0$.

$$|y_0| \geq s\beta|\omega_2||x^k| - |a||x| - |z|.$$

Using Equation (3), we obtain

$$\begin{aligned}|y_0| &\geq s\beta|\omega_2||z^k| - |a||z| - |z|, \quad (s, \beta \in (0,1]) \\ &\geq |z|[s\beta|\omega_2||z^{k-1}| - (1 + |a|)].\end{aligned}$$

Since

$$|z| > (\frac{2 + |a|}{s\beta|\omega_2|})^{\frac{1}{k-1}},$$

implies that

$$|y_0| \geq |z|. \tag{4}$$

Now, for the last step of the four-step iteration,

$$|z_{k+1}| = |(1-\alpha)^s z_k + \alpha^s T(y_k)|.$$

Again, if $k = 0$, $z_0 = z$, and $y_0 = y$

$$\begin{aligned}
|z_1| &= |(1-\alpha)^s z + \alpha^s T(y)| \\
&= |(1-\alpha)^s z + \alpha^s(\cos(y^k) + ay + c)|,\ (\alpha, s \in (0,1],\ so\ \ \alpha^s \geq s\alpha) \\
&\geq |(1-\alpha)^s z + s\alpha(\cos(y^k) + ay + c)| \\
&\geq |s\alpha(\cos(y^k) + ay) + (1-\alpha)^s z| - s\alpha|c| \\
&\geq |s\alpha(\cos(y^k) + ay) + (1-\alpha)^s z| - s\alpha|z|,\ \ (|z| \geq |c|), \\
&\geq |s\alpha(\cos(y^k) + ay)| - |(1-\alpha)^s z| - s\alpha|z|.
\end{aligned}$$

Expanding $(1-\alpha)^s$ utilizing a binomial theorem up to linear terms of $\alpha$, we attain

$$\begin{aligned}
|z_1| &\geq |s\alpha(\cos(y^k) + ay)| - |(1-s\alpha)z| - s\alpha|z| \\
&\geq |s\alpha(\cos(y^k) + ay)| - |z| + |s\alpha z| - s\alpha|z| \\
&\geq s\alpha|\cos(y^k)| - s\alpha|a||y| - |z| \\
&\geq s\alpha|\cos(y^k)| - |a||y| - |z|,\ \ s, \alpha \in (0,1].
\end{aligned}$$

Since

$$|\cos(y^k)| = |1 - \frac{y^{2k}}{2!} + \frac{y^{4k}}{4!} - \dots| \geq |\omega_1||y^k|,$$

where $|\omega_1| \in (0,1]$ except the value of $y$ for which $|\omega_1| = 0$, then

$$|z_1| \geq s\alpha|\omega_1||y^k| - |a||y| - |z|.$$

Using Equation (4),

$$\begin{aligned}
|z_1| &\geq s\alpha|\omega_1||z^k| - |a||z| - |z|,\ \ (s, \alpha, \omega_1 \in (0,1]) \\
&\geq |z|[s\alpha|\omega_1||z^{k-1}| - (1+|a|)].
\end{aligned}$$

For $k = 1$,

$$\begin{aligned}
|z_2| &\geq |z_1|[s\alpha|\omega_1||z^{k-1}| - (1+|a|)] \\
&\geq |z|(s\alpha|\omega_1||z^{k-1}| - (1+|a|))^2.
\end{aligned}$$

On iterating until the $k^{th}$ term,

$$\begin{aligned}
|z_3| &\geq |z|[s\alpha|\omega_1||z^{k-1}| - (1+|a|)]^3 \\
|z_4| &\geq |z|[s\alpha|\omega_1||z^{k-1}| - (1+|a|)]^4 \\
&. \\
&. \\
&. \\
|z_k| &\geq |z|[s\alpha|\omega_1||z^{k-1}| - (1+|a|)]^k.
\end{aligned}$$

Since $|z| \geq |c| > (\frac{2+|a|}{s\alpha|\omega_1|})^{\frac{1}{k-1}}$, where $|\omega_1| \in (0,1]$, this implies

$$|z_k| \geq |z|,$$

that is, $|z_k| \to \infty$ as $k \to \infty$. □

**Corollary 1.** *Suppose that* $|z_m| > \max\left\{|c|, (\frac{2+|a|}{s\alpha|\omega_1|})^{\frac{1}{k-1}}, (\frac{2+|a|}{s\beta|\omega_2|})^{\frac{1}{k-1}}, (\frac{2+|a|}{s\gamma|\omega_3|})^{\frac{1}{k-1}}, (\frac{2+|a|}{s\delta|\omega_4|})^{\frac{1}{k-1}}\right\}$, $m > 0$.
*Since* $s\alpha|\omega_1||z^{k-1}| - (1+|a|) > 1$ *and* $|z_{m+k}| > |z|(s\alpha|\omega_1||z^{k-1}| - (1+|a|))^{m+k}$, *then* $|z_k| \to \infty$ *when* $k \to \infty$.

**Remark 1.** *Corollary 1 gives escape radii for generating some new Julia and Mandelbrot sets of complex-valued cosine functions via a four-step iteration scheme extended with s-convexity.*

**Remark 2.** *Theorem 1 gives the escape criterion for complex cosine functions via*
1. *Noor iteration scheme extended with s-convexity [29] when* $\delta = 0$.
2. *Ishikawa iteration extended with s-convexity [30] when* $\gamma, \delta = 0$.
3. *Mann iteration scheme extended with s-convexity when* $\beta, \gamma, \delta = 0$.
4. *Picard iteration scheme extended with s-convexity when* $\beta, \gamma, \delta = 0$ *and* $\alpha = 1$.
5. *Noor iteration scheme [7] when* $\delta = 0$ *and* $s = 1$.
6. *Ishikawa iteration scheme [5] when* $\gamma, \delta = 0$, *and* $s = 1$.
7. *Mann iteration scheme [6] when* $\beta, \gamma, \delta = 0$, *and* $s = 1$.
8. *Picard iteration scheme [8] when* $\beta, \gamma, \delta = 0, \alpha = 1$, *and* $s = 1$.

**Remark 3.** *In Theorem 1, we obtained escape criteria via a four-step iteration scheme extended with s-convexity for a cosine function* $T(z) = cos(z^k) + az + c;\ a,\ c \in \mathbb{C},\ k \geq 1$ *using the inequalities* $\alpha^s \geq s\alpha;\ \beta^s \geq s\beta;\ \gamma^s \geq s\gamma;\ \delta^s \geq s\delta;\ -(1-\alpha)s \geq -(1-s\alpha);\ -(1-\beta)s \geq -(1-s\beta);\ -(1-\gamma)s \geq -(1-s\gamma)$ *and* $-(1-\delta)s \geq -(1-s\delta)$; *which are true in* $(0,1]$. *On the contrary, Nazeer et al. [31] established the escape criteria via Jungck–Mann and Jungck–Ishikawa fixed-point iterations extended with s-convexity for a complex-valued polynomial* $f(z) = z^k - az + c, a,\ c \in \mathbb{C},\ k \geq 1$ *without generating the fractals using the binomial theorem up to linear terms which do not hold in* $(0,1]$ *for the involved parameters. One may verify that none of the inequalities* $-(1-\alpha)s \geq -(1-s\alpha);\ -(1-\beta)s \geq -(1-s\beta);\ (1-(1-\alpha))^s \geq 1-s(1-\alpha);\ (1-(1-\beta))^s \geq 1-s(1-\beta);$ *hold in* $(0,1]$. *Similar errors were noticed in the proof of theorems for establishing escape criteria for complex-valued polynomials extended with convexity parameters, in Gdawiec [32], Kang et al. [33], Kumari et al. [34], Li et al. [35], Kwun et al. [36], Nazeer et al. [31], and many others. Furthermore, Nazeer et al. [31] asserted their error following the principle of mathematical induction in Theorem 4.9 (Theorem 3.9). However, the authors used Theorems 4.1 and 4.5 (Theorems 3.1 and 3.5) to prove the initial steps. After this, they made an inductive assumption, which is not used in the proof for* $(n+1)$. *Consequently, Nazeer et al. [31] did not utilize the principle of mathematical induction and their assertion is false. For recent improved work in this direction, see Antal et al. [37], Tomar et al. [38], and the references therein.*

## 3. Generation of Fractals

We used Algorithm 1 (Geometry of Julia set) and Algorithm 2 (Geometry of Mandelbrot set), for sketching aesthetic fractals for complex cosine functions using a four-step iteration scheme extended with s-convexity via MATLAB 9.1.0 (R2016b). We also developed a colourmap (Figure 1). Throughout this process, we attained many fractals and mostly these generated fractals as Julia and Mandelbrot sets have symmetry. We only cover the behaviour of selected fractals for the various parameter values using at most K = 30 iterations.

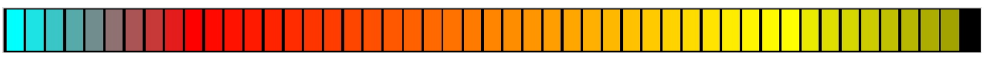

**Figure 1.** Colourmap used in sketching the fractals.

**Algorithm 1:** Geometry of Julia Set

Input: $T(z) = \cos(z^k) + az + c, k \geq 2;\ a, c \in \mathbb{C},\ A \subset \mathbb{C}$-area; $K$-maximum number of iterations; $\alpha, \beta, \gamma, \delta \in (0, 1]$-parameters of four-step iteration with colourmap [0..C−0]-colour with C colours.

Output: Julia set for area A.

**for** $z_0 \in A$ **do**

$R_1 = (\frac{2+|a|}{s\alpha|\omega_1|})^{\frac{1}{k-1}}$

$R_2 = (\frac{2+|a|}{s\beta|\omega_2|})^{\frac{1}{k-1}}$

$R_3 = (\frac{2+|a|}{s\gamma|\omega_3|})^{\frac{1}{k-1}}$

$R_4 = (\frac{2+|a|}{s\delta|\omega_4|})^{\frac{1}{k-1}}$

$R = \max\{|c|, R_1, R_2, R_3, R_4\}$

$k = 0$

$z_0 = 0$

**while** $n \geq K$ **do**

$w_k = (1-\delta)^s z_k + \delta^s T z_k$

$x_k = (1-\gamma)^s z_k + \gamma^s T w_k$

$y_k = (1-\beta)^s z_k + \beta^s T x_k$

$z_{k+1} = (1-\alpha)^s z_k + \alpha^s T y_k$

**if** $|z_{k+1} > R|$ **then**

  break

**end if**

$k = k + 1$

**end while**

$i = [(C-1)\frac{k}{K}]$

colour $z_0$ with colourmap $[i]$

**end for**

### *3.1. Julia Sets*

We obtain stunning fractals for different parameters, as given in Table 1, which are symmetrical with regard to the initial line (as can be seen in Figure 2). We notice that, as the value of the parameter $k$ increases, the amount of black colour in the Julia set decreases and the red colour increases. Furthermore, the area employed by the Julia set decreases, and the time taken to generate it increases with the increase in the value of parameter $k$. However, smaller values of parameter $k$ add beauty to the Julia set and larger values make it circular.

**Table 1.** The parameters used in Figure 2.

| Sr. No. | a | c | s | $\alpha$ | $\beta$ | $\gamma$ | $\delta$ | $\omega_1$ | $\omega_2$ | $\omega_3$ | $\omega_4$ | k |
|---|---|---|---|---|---|---|---|---|---|---|---|---|
| (a) | 1.0 | 1.9 | 0.5656 | 0.0093 | 0.0095 | 0.0055 | 0.0057 | 0.6204 | 0.5221 | 0.9449 | 0.7777 | 2 |
| (b) | 1.0 | 1.9 | 0.5656 | 0.0093 | 0.0095 | 0.0055 | 0.0057 | 0.6204 | 0.5221 | 0.9449 | 0.7777 | 3 |
| (c) | 1.0 | 1.9 | 0.5656 | 0.0093 | 0.0095 | 0.0055 | 0.0057 | 0.6204 | 0.5221 | 0.9449 | 0.7777 | 4 |
| (d) | 1.0 | 1.9 | 0.5656 | 0.0093 | 0.0095 | 0.0055 | 0.0057 | 0.6204 | 0.5221 | 0.9449 | 0.7777 | 8 |
| (e) | 1.0 | 1.9 | 0.5656 | 0.0093 | 0.0095 | 0.0055 | 0.0057 | 0.6204 | 0.5221 | 0.9449 | 0.7777 | 10 |
| (f) | 1.0 | 1.9 | 0.5656 | 0.0093 | 0.0095 | 0.0055 | 0.0057 | 0.6204 | 0.5221 | 0.9449 | 0.7777 | 20 |

**Algorithm 2:** Geometry of Mandelbrot Set

Input: $T(z) = \cos(z^k) + az + c,\ k \geq 2;\ a, c \in \mathbb{C},\ A \subset \mathbb{C}$-area; $K$-maximum number of iterations; $\alpha, \beta, \gamma, \delta \in (0, 1]$-parameters of four-step iteration with colourmap [0..C−0]-colour with C colours.
Output: Mandelbrot set for area A.
**for** $c \in A$ **do**
$R_1 = (\frac{2+|a|}{s\alpha|\omega_1|})^{\frac{1}{k-1}}$
$R_2 = (\frac{2+|a|}{s\beta|\omega_2|})^{\frac{1}{k-1}}$
$R_3 = (\frac{2+|a|}{s\gamma|\omega_3|})^{\frac{1}{k-1}}$
$R_4 = (\frac{2+|a|}{s\delta|\omega_4|})^{\frac{1}{k-1}}$
$R = \max\{|c|, R_1, R_2, R_3, R_4\}$
$k = 0$
**while** $n \geq K$ **do**
$w_k = (1-\delta)^s z_k + \delta^s T z_k$
$x_k = (1-\gamma)^s z_k + \gamma^s T w_k$
$y_k = (1-\beta)^s z_k + \beta^s T x_k$
$z_{k+1} = (1-\alpha)^s z_k + \alpha^s T y_k$
**if** $|z_{k+1} > R|$ **then**
break
**end if**
$k = k + 1$
**end while**
$i = [(C-1)\frac{k}{K}]$
colour $z_0$ with colourmap $[i]$
**end for**

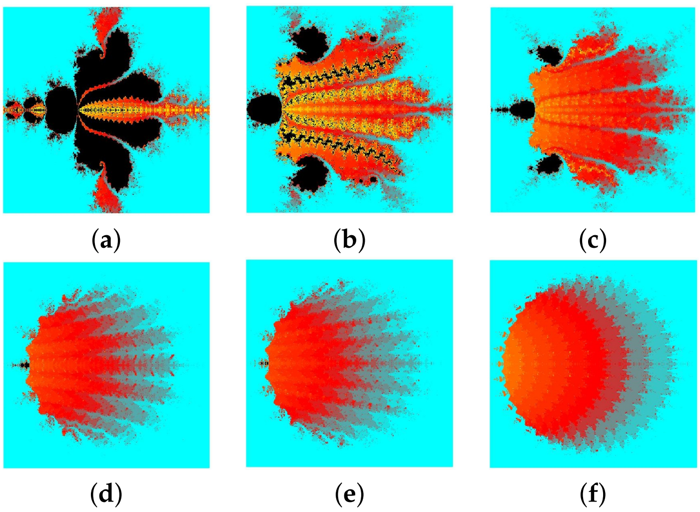


**Figure 2.** Effect of $k$ on the Julia set in four-step iteration extended with s-convexity. (**a**) area [−4.5, 4] × [−3, 3] and time 0.77 s. (**b**) Area [−2, 2] × [−2, 2] and time 0.89 s. (**c**) Area [−2, 1.5] × [−1.8, 1.8] and time 0.97 s. (**d**) [−1.5, 1.5] × [−1.5, 1.5] and time 0.97 s. (**e**) [−1.4, 1.4] × [−1.4, 1.4] and time 1.17 s. (**f**) [−1.3, 1.3] × [−1.3, 1.3] and time 1.25 s.

We observe that, for real values of parameter $a$, we obtain Julia sets that are symmetrical with respect to the initial line (as can be seen in Figure 3a–c). As the value of the real parameter $a$ increases, the amount of black colour in the Julia set decreases and the red colour increases. Furthermore, the area occupied by the Julia set and the time taken to generate it decreases with the increase in value of $a$. However, complex values of parameter

$a$ give a twist to the Julia set and it no longer remains symmetrical with respect to the initial line (see, Table 2 and Figure 3).

**Table 2.** The parameters used in Figure 3.

| Sr. No. | a | c | s | $\alpha$ | $\beta$ | $\gamma$ | $\delta$ | $\omega_1$ | $\omega_2$ | $\omega_3$ | $\omega_4$ | k |
|---|---|---|---|---|---|---|---|---|---|---|---|---|
| (a) | 1.5 | 1.9 | 0.5656 | 0.0093 | 0.0095 | 0.0055 | 0.0057 | 0.6204 | 0.5221 | 0.9449 | 0.7777 | 2 |
| (b) | 2.0 | 1.9 | 0.5656 | 0.0093 | 0.0095 | 0.0055 | 0.0057 | 0.6204 | 0.5221 | 0.9449 | 0.7777 | 2 |
| (c) | 4.0 | 1.9 | 0.5656 | 0.0093 | 0.0095 | 0.0055 | 0.0057 | 0.6204 | 0.5221 | 0.9449 | 0.7777 | 2 |
| (d) | 1 + 2.3i | 1.9 | 0.5656 | 0.0093 | 0.0095 | 0.0055 | 0.0057 | 0.6204 | 0.5221 | 0.9449 | 0.7777 | 2 |
| (e) | 1.5 − 2i | 1.9 | 0.5656 | 0.0093 | 0.0095 | 0.0055 | 0.0057 | 0.6204 | 0.5221 | 0.9449 | 0.7777 | 2 |
| (f) | 5i | 1.9 | 0.5656 | 0.0093 | 0.0095 | 0.0055 | 0.0057 | 0.6204 | 0.5221 | 0.9449 | 0.7777 | 2 |

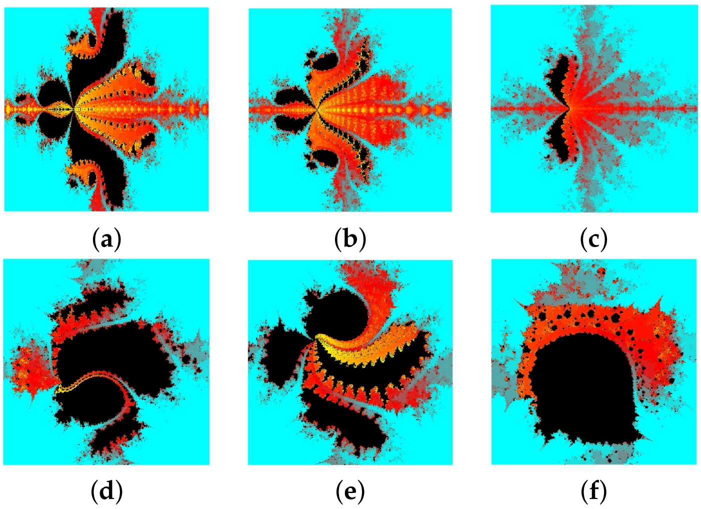

**Figure 3.** Effect of $a$ on Julia set in four-step iteration extended with s-convexity. (**a**) Area $[-4, 3.5] \times [-3, 3]$ and time 1.02 s. (**b**) Area $[-3.5, 3.5] \times [-3, 3]$ and time 0.97 s. (**c**) Area $[-3, 3] \times [-3, 3]$ and time 0.95 s. (**d**) Area $[-3, 3] \times [-3, 3]$ and time 0.92 s. (**e**) Area $[-3, 2.5] \times [-2.5, 2.5]$ and time 0.90 s. (**f**) Area $[-2.5, 2.5] \times [-2.5, 2.5]$ and time 0.87 s.

We observe that we obtain twisted Julia sets for complex values of $c$, while we obtain Julia sets that are symmetrical with respect to the initial line for real values of $c$. Larger absolute values of $c$ add redness (see, Table 3 and Figure 4).

**Table 3.** The parameters used in Figure 4.

| Sr. No. | a | c | s | $\alpha$ | $\beta$ | $\gamma$ | $\delta$ | $\omega_1$ | $\omega_2$ | $\omega_3$ | $\omega_4$ | k |
|---|---|---|---|---|---|---|---|---|---|---|---|---|
| (a) | 2.0 | 0 | 0.5656 | 0.0093 | 0.0095 | 0.0055 | 0.0057 | 0.6204 | 0.5221 | 0.9449 | 0.7777 | 2 |
| (b) | 2.0 | 2.5 | 0.5656 | 0.0093 | 0.0095 | 0.0055 | 0.0057 | 0.6204 | 0.5221 | 0.9449 | 0.7777 | 2 |
| (c) | 2.0 | i | 0.5656 | 0.0093 | 0.0095 | 0.0055 | 0.0057 | 0.6204 | 0.5221 | 0.9449 | 0.7777 | 2 |
| (d) | 2.0 | 2i | 0.5656 | 0.0093 | 0.0095 | 0.0055 | 0.0057 | 0.6204 | 0.5221 | 0.9449 | 0.7777 | 2 |

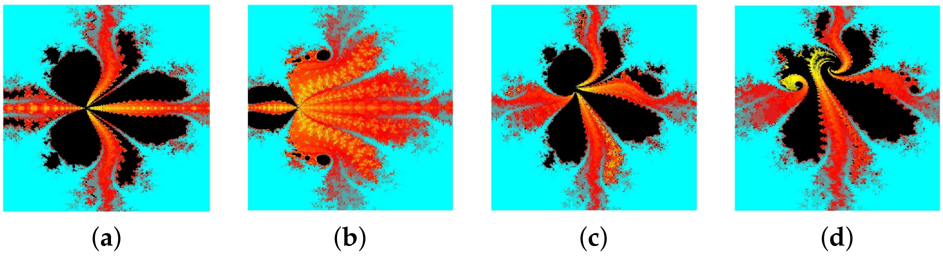

**Figure 4.** Effect of $c$ on Julia set in four-step iteration extended with s-convexity. (**a**) Area $[-2, 1.5] \times [-1.8, 1.8]$ and time 0.97 s. (**b**) Area $[-2.5, 2.5] \times [-3, 3]$ and time 0.94 s. (**c**) Area $[-3, 3] \times [-3, 3]$ and time 1.02 s. (**d**) Area $[-2.5, 2.5] \times [-3, 3]$ and time 0.98 s.

The smaller values of the convexity parameter $s$ add beauty to the Julia set which occupies a smaller area and takes less time to generate. The black colour starts appearing with the increase in the value of $s$ (see, Table 4 and Figure 5).

**Table 4.** The parameters used in Figure 5.

| Sr. No. | a | c | s | $\alpha$ | $\beta$ | $\gamma$ | $\delta$ | $\omega_1$ | $\omega_2$ | $\omega_3$ | $\omega_4$ | k |
|---|---|---|---|---|---|---|---|---|---|---|---|---|
| (a) | 2.0 | 1.9 | 0.1919 | 0.0093 | 0.0095 | 0.0055 | 0.0057 | 0.6204 | 0.5221 | 0.9449 | 0.7777 | 2 |
| (b) | 2.0 | 1.9 | 0.2929 | 0.0093 | 0.0095 | 0.0055 | 0.0057 | 0.6204 | 0.5221 | 0.9449 | 0.7777 | 2 |
| (c) | 2.0 | 1.9 | 0.3939 | 0.0093 | 0.0095 | 0.0055 | 0.0057 | 0.6204 | 0.5221 | 0.9449 | 0.7777 | 2 |
| (d) | 2.0 | 1.9 | 0.4949 | 0.0093 | 0.0095 | 0.0055 | 0.0057 | 0.6204 | 0.5221 | 0.9449 | 0.7777 | 2 |

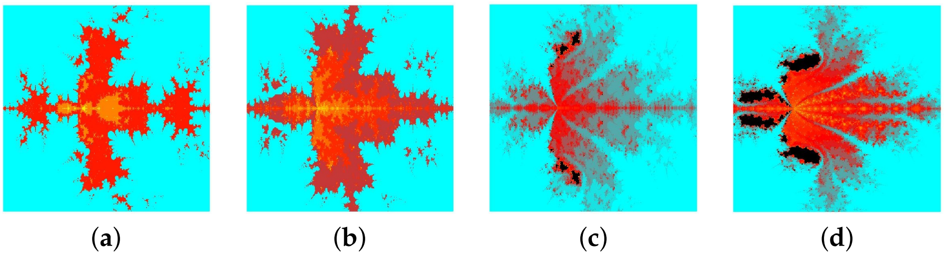

**Figure 5.** Effect of $s$ on Julia set in four-step iteration extended with s-convexity. (**a**) Area $[-3, 2] \times [-2, 2]$ and time 0.95 s. (**b**) Area $[-3, 2.5] \times [-2, 2]$ and time 1.03 s. (**c**) Area $[-3, 2.7] \times [-2, 2]$ and time 1.05 s. (**d**) Area $[-3, 3] \times [-2, 2]$ and time 1.07 s.

The smaller value of parameter $\alpha$ of the four-step iteration adds beauty to the Julia set, which occupies a larger area and takes more time to generate. When the value of $\alpha$ reaches 1, Julia set becomes very feeble and red. On the other hand, as $\alpha$ approaches 0, the Julia set turns completely black (see, Table 5 and Figure 6).

**Table 5.** The parameters used in Figure 6.

| Sr. No. | a | c | s | $\alpha$ | $\beta$ | $\gamma$ | $\delta$ | $\omega_1$ | $\omega_2$ | $\omega_3$ | $\omega_4$ | k |
|---|---|---|---|---|---|---|---|---|---|---|---|---|
| (a) | 2.0 | 1.9 | 0.5656 | 0.0012 | 0.0095 | 0.0055 | 0.0057 | 0.6204 | 0.5221 | 0.9449 | 0.7777 | 2 |
| (b) | 2.0 | 1.9 | 0.5656 | 0.0121 | 0.0095 | 0.0055 | 0.0057 | 0.6204 | 0.5221 | 0.9449 | 0.7777 | 2 |
| (c) | 2.0 | 1.9 | 0.5656 | 0.1212 | 0.0095 | 0.0055 | 0.0057 | 0.6204 | 0.5221 | 0.9449 | 0.7777 | 2 |
| (d) | 2.0 | 1.9 | 0.5656 | 1.0 | 0.0095 | 0.0055 | 0.0057 | 0.6204 | 0.5221 | 0.9449 | 0.7777 | 2 |

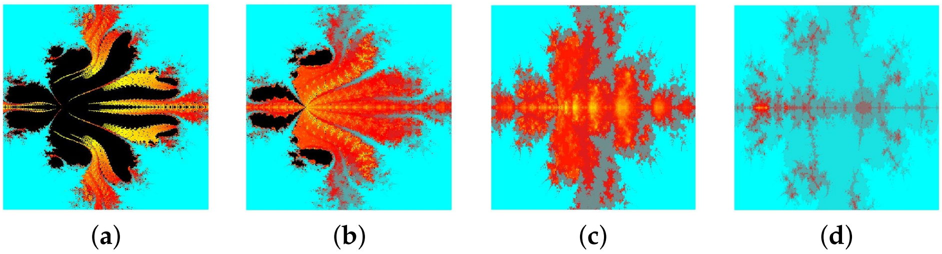


**Figure 6.** Effect of $\alpha$ on Julia set in four-step iteration extended with s-convexity. (**a**) Area [−3.5, 3.5] × [−3, 3] and time 1.01 s. (**b**) Area [−3.5, 3.5] × [−2.5, 2.5] and time 0.99 s. (**c**) Area [−3.5, 3.5] × [−2.4, 2.4] and time 0.96 s. (**d**) Area [−3, 3] × [−2, 2] and time 0.94 s.

The smaller value of parameter $\beta$ of the four-step iteration adds beauty to the Julia set which occupies a larger area and takes more time to generate. The value of $\beta$ nearer to 1 makes the Julia set very feeble and red (see, Table 6 and Figure 7).

**Table 6.** The parameters used in Figure 7.

| Sr. No. | a | c | s | $\alpha$ | $\beta$ | $\gamma$ | $\delta$ | $\omega_1$ | $\omega_2$ | $\omega_3$ | $\omega_4$ | k |
|---|---|---|---|---|---|---|---|---|---|---|---|---|
| (a) | 2.0 | 1.9 | 0.5656 | 0.0093 | 0.0000 | 0.0055 | 0.0057 | 0.6204 | 0.5221 | 0.9449 | 0.7777 | 2 |
| (b) | 2.0 | 1.9 | 0.5656 | 0.0093 | 0.2525 | 0.0055 | 0.0057 | 0.6204 | 0.5221 | 0.9449 | 0.7777 | 2 |
| (c) | 2.0 | 1.9 | 0.5656 | 0.0093 | 0.4545 | 0.0055 | 0.0057 | 0.6204 | 0.5221 | 0.9449 | 0.7777 | 2 |
| (d) | 2.0 | 1.9 | 0.5656 | 0.0093 | 0.8585 | 0.0055 | 0.0057 | 0.6204 | 0.5221 | 0.9449 | 0.7777 | 2 |

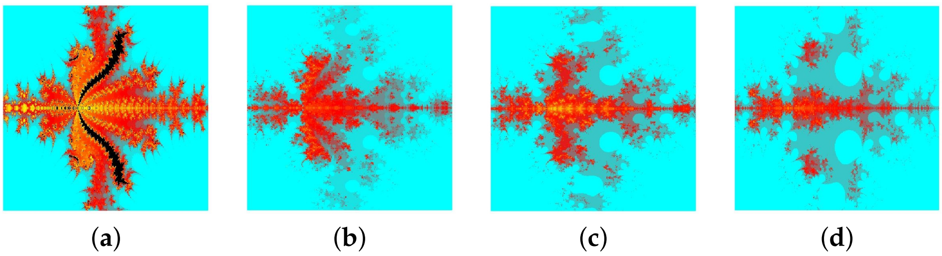


**Figure 7.** Effect of $\beta$ on Julia set in four-step iteration extended with s-convexity. (**a**) Area [−4.2, 4.2] × [−3, 3] and time 1.07 s. (**b**) Area [−3.5, 3.5] × [−2.9, 2.9] and time 1.06 s. (**c**) Area [−3.5, 3.5] × [−2.9, 2.9] and time 1.06 s. (**d**) Area [−3, 3] × [−2.5, 2.5] and time 0.96 s.

The parameters $\gamma$ and $\delta$ also follow the pattern of $\alpha$ and $\beta$ (see, Tables 7 and 8 and Figures 8 and 9 respectively).

**Table 7.** The parameters used in Figure 8.

| Sr. No. | a | c | s | $\alpha$ | $\beta$ | $\gamma$ | $\delta$ | $\omega_1$ | $\omega_2$ | $\omega_3$ | $\omega_4$ | k |
|---|---|---|---|---|---|---|---|---|---|---|---|---|
| (a) | 2.0 | 1.9 | 0.5656 | 0.0093 | 0.0095 | 0.0000 | 0.0057 | 0.6204 | 0.5221 | 0.9449 | 0.7777 | 2 |
| (b) | 2.0 | 1.9 | 0.5656 | 0.0093 | 0.0095 | 0.0011 | 0.0057 | 0.6204 | 0.5221 | 0.9449 | 0.7777 | 2 |
| (c) | 2.0 | 1.9 | 0.5656 | 0.0093 | 0.0095 | 0.0222 | 0.0057 | 0.6204 | 0.5221 | 0.9449 | 0.7777 | 2 |
| (d) | 2.0 | 1.9 | 0.5656 | 0.0093 | 0.0095 | 0.3333 | 0.0057 | 0.6204 | 0.5221 | 0.9449 | 0.7777 | 2 |

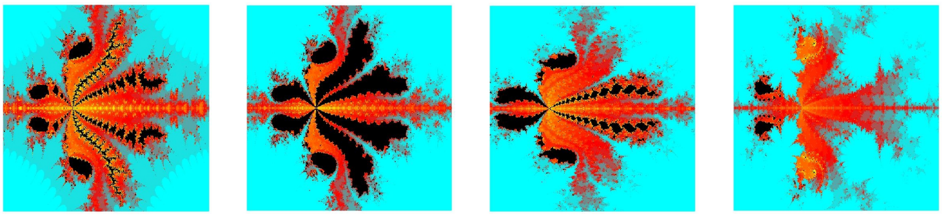

(**a**) (**b**) (**c**) (**d**)

**Figure 8.** Effect of $\gamma$ on Julia set in four-step iteration extended with s-convexity. (**a**) Area $[-3.5, 3.5] \times [-2.5, 2.5]$ and time 0.78 s. (**b**) Area $[-3.3, 3.3] \times [-2.7, 2.7]$ and time 0.76 s. (**c**) Area $[-3, 3] \times [-2.7, 2.7]$ and time 0.76 s. (**d**) Area $[-2, 1.5] \times [-1.8, 1.8]$ and time 0.72 s.

Note that for larger values of $\delta$, the basic shape of the Julia set remains the same. However, Julia set shrinks and becomes red (see, Table 8 and Figure 9).

**Table 8.** The parameters used in Figure 9.

| Sr. No. | a | c | s | $\alpha$ | $\beta$ | $\gamma$ | $\delta$ | $\omega_1$ | $\omega_2$ | $\omega_3$ | $\omega_4$ | k |
|---|---|---|---|---|---|---|---|---|---|---|---|---|
| (a) | 2.0 | 1.9 | 0.5656 | 0.0093 | 0.0095 | 0.0055 | 0.001243 | 0.6204 | 0.5221 | 0.9449 | 0.7777 | 2 |
| (b) | 2.0 | 1.9 | 0.5656 | 0.0093 | 0.0095 | 0.0055 | 0.005242 | 0.6204 | 0.5221 | 0.9449 | 0.7777 | 2 |
| (c) | 2.0 | 1.9 | 0.5656 | 0.0093 | 0.0095 | 0.0055 | 0.04949 | 0.6204 | 0.5221 | 0.9449 | 0.7777 | 2 |
| (d) | 2.0 | 1.9 | 0.5656 | 0.0093 | 0.0095 | 0.0055 | 0.221159 | 0.6204 | 0.5221 | 0.9449 | 0.7777 | 2 |

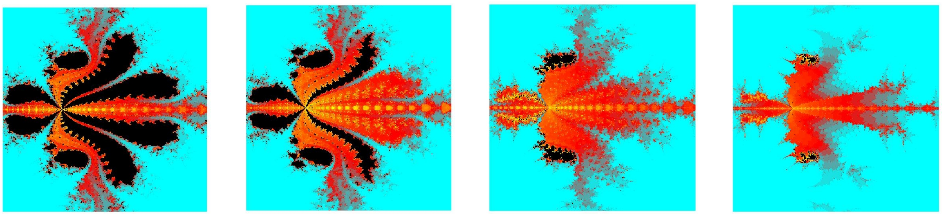

(**a**) (**b**) (**c**) (**d**)

**Figure 9.** Effect of $\delta$ on Julia set in four-step iteration extended with $s$-convexity. (**a**) Area $[-3.5, 3.5] \times [-2.7, 2.7]$ and time 0.77 s. (**b**) Area $[-2, 2] \times [-2, 2]$ and time 0.76 s. (**c**) Area $[-2, 1.5] \times [-1.8, 1.8]$ and time 0.73 s. (**d**) Area $[-2, 1.5] \times [-1.8, 1.8]$ and time 0.73 s.

In view of Remark 2, Figure 10a–d represent the quintic Julia sets corresponding to four-step iteration extended with s-convexity, Noor iteration extended with s-convexity (three-step), Ishikawa iteration extended with s-convexity (two-step), and Mann iteration extended with s-convexity (one -step), respectively (as can be seen in Table 9). We observe that as we move from a four-step iteration extended with s-convexity to a one-step iteration extended with s-convexity, the amount of red colour decreases while the black colour increases. The number of outer spikes is 2k in each. However, the quintic Julia fractal is sharper for one-step iteration.

**Table 9.** The parameters used in Figures 10–12.

| Sr. No. | a | c | s | $\alpha$ | $\beta$ | $\gamma$ | $\delta$ | $\omega_1$ | $\omega_2$ | $\omega_3$ | $\omega_4$ | k |
|---|---|---|---|---|---|---|---|---|---|---|---|---|
| (a) | 2.5 | 1.5i | 0.6565 | 0.0050 | 0.0069 | 0.0072 | 0.0045 | 0.4856 | 0.8935 | 0.3932 | 0.3454 | 5 |
| (b) | 2.5 | 1.5i | 0.6565 | 0.0050 | 0.0069 | 0.0072 | 0.0 | 0.4856 | 0.8935 | 0.3932 | - | 5 |
| (c) | 2.5 | 1.5i | 0.6565 | 0.0050 | 0.0069 | 0.0 | 0.0 | 0.4856 | 0.8935 | - | - | 5 |
| (d) | 2.5 | 1.5i | 0.6565 | 0.0050 | 0.0 | 0.0 | 0.0 | 0.4856 | - | - | - | 5 |

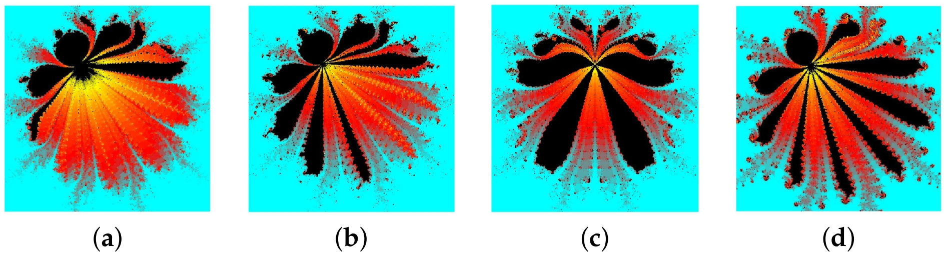

**Figure 10.** Effect of different iterations extended with s-convexity on Julia set (four-step, Noor, Ishikawa, and Mann iterations). (**a**) Area [−1.5, 1.5] × [−1.8, 1.8] and time 1.35 s. (**b**) Area [−1.5, 1.5] × [−1.5, 1.7] and time 1.24 s. (**c**) Area [−1.5, 1.5] × [−1.5, 1.5] and time 1.11 s. (**d**) Area [−1.5, 1.5] × [−1.5, 1.5] and time 0.85 s.

For $s = 1$ in Table 9, all the quintic Julia sets turn black and are almost similar in shape with 10 spikes (2k) for all standard four-step, Noor, Ishikawa, and Mann iterations. Although other colours start appearing, the time of generation the occupied area decreases as we move from a four-step to a one-step iteration (on removing convexity) (see, Figure 11).

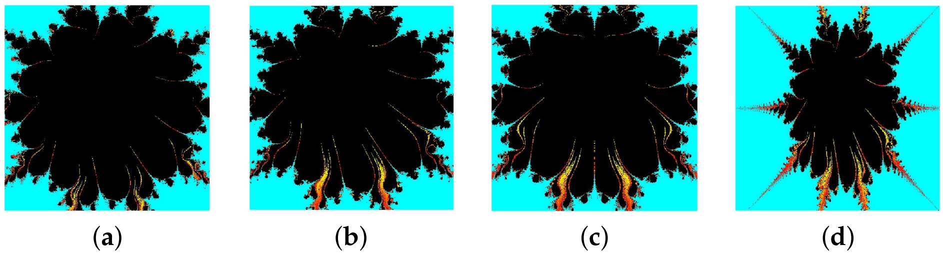

**Figure 11.** Effect of different standard four-step, Noor, Ishikawa, and Mann iterations on Julia set. (**a**) Area [−1.5, 1.5] × [−1.8, 1.8] and time 1.23 s. (**b**) Area [−1.5, 1.5] × [−1.5, 1.7] and time 1.18 s. (**c**) Area [−1.5, 1.5] × [−1.5, 1.5] and time 1.00 s. (**d**) Area [−1.5, 1.5] × [−1.5, 1.5] and time 0.95 s.

As we move from a four-step iteration to a one-step iteration (Picard) using the parameters of Table 9, we obtain an entirely different red-coloured quintic Julia set (as can be seen in Remark 2: $\alpha = 1; \beta = \gamma = \delta = 0$). Its shape remains the shape even if the Picard iteration is not extended with s-convexity ($s = 1$) (see, Figure 12).

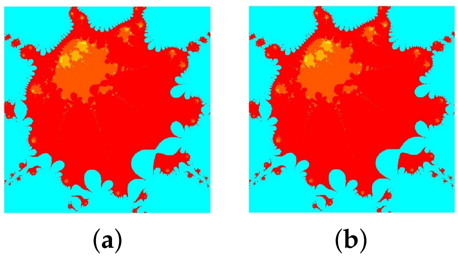

**Figure 12.** Effect of Picard iteration extended with s-convexity and standard Picard iteration $(s = 1)$ on the quintic Julia set. (**a**) Area [−1.5, 1.5] × [−1.5, 1.5] and time 1.11 s. (**b**) Area [−1.5, 1.5] × [−1.5, 1.5] and time 1.14 s.

### 3.2. Mandelbrot Sets

As the value of $k$ increases, the number of petals increases, and for $k = 5$, the Mandelbrot set takes the shape of a lotus (see, Table 10 and Figure 13).

**Table 10.** The parameters used in Figure 13.

| Sr. No. | a | s | $\alpha$ | $\beta$ | $\gamma$ | $\delta$ | $\omega_1$ | $\omega_2$ | $\omega_3$ | $\omega_4$ | k |
|---|---|---|---|---|---|---|---|---|---|---|---|
| (a) | 0.4949 | 0.5151 | 0.0078 | 0.0056 | 0.0995 | 0.0312 | 0.8383 | 0.0119 | 0.7474 | 0.6556 | 2 |
| (b) | 0.4949 | 0.5151 | 0.0078 | 0.0056 | 0.0995 | 0.0312 | 0.8383 | 0.0119 | 0.7474 | 0.6556 | 3 |
| (c) | 0.4949 | 0.5151 | 0.0078 | 0.0056 | 0.0995 | 0.0312 | 0.8383 | 0.0119 | 0.7474 | 0.6556 | 4 |
| (d) | 0.4949 | 0.5151 | 0.0078 | 0.0056 | 0.0995 | 0.0312 | 0.8383 | 0.0119 | 0.7474 | 0.6556 | 5 |

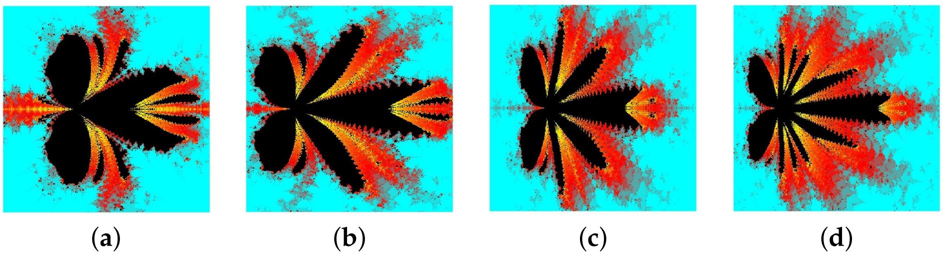

**Figure 13.** Effect of $k$ on the Mandelbrot set in four-step iteration extended with s-convexity. (**a**) Area $[-2, 2] \times [-2, 2]$ and time 0.86 s. (**b**) Area $[-1.2, 1.2] \times [-1.4, 1.4]$ and time 0.99 s. (**c**) Area $[-1.5, 1.5] \times [-1, 1]$ and time 1.08 s. (**d**) Area $[-1.2, 1.2] \times [-0.9, 0.9]$ and time 1.09 s.

If the absolute value of parameter $a$ increases, the redness in the Mandelbrot set also increases. For real values of $a$, we obtain Mandelbrot sets those are symmetrical with respect to the real line, and for complex values, these start to become twisted and resemble a swirl for $a = 5i$ (see, Table 11 and Figure 14).

**Table 11.** The parameters used in Figure 14.

| Sr. No. | a | s | $\alpha$ | $\beta$ | $\gamma$ | $\delta$ | $\omega_1$ | $\omega_2$ | $\omega_3$ | $\omega_4$ | k |
|---|---|---|---|---|---|---|---|---|---|---|---|
| (a) | 0.0 | 0.5151 | 0.0078 | 0.0056 | 0.0995 | 0.0312 | 0.8383 | 0.0119 | 0.7474 | 0.6556 | 2 |
| (b) | 1.4949 | 0.5151 | 0.0078 | 0.0056 | 0.0995 | 0.0312 | 0.8383 | 0.0119 | 0.7474 | 0.6556 | 2 |
| (c) | 0.3939i | 0.5151 | 0.0078 | 0.0056 | 0.0995 | 0.0312 | 0.8383 | 0.0119 | 0.7474 | 0.6556 | 2 |
| (d) | 5i | 0.5151 | 0.0078 | 0.0056 | 0.0995 | 0.0312 | 0.8383 | 0.0119 | 0.7474 | 0.6556 | 2 |

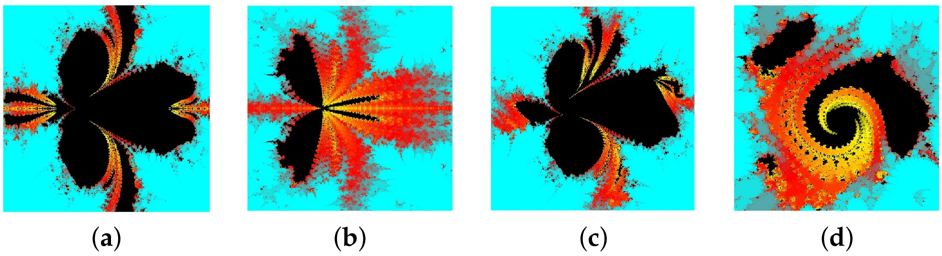

**Figure 14.** Effect of $a$ on Mandelbrot set in four-step iteration extended with s-convexity. (**a**) Area $[-2.2, 2.2] \times [-2.4, 2.4]$ and time 0.89 s. (**b**) Area $[-1.5, 1.5] \times [-1.8, 1.8]$ and time 0.87 s. (**c**) Area $[-2.5, 2.2] \times [-2.3, 2.3]$ and time 0.85 s. (**d**) Area $[-1.3, 1.1] \times [-1.3, 1.3]$ and time 0.88 s.

If the values of convexity parameter $s$ increase, then the area occupied by the Mandelbrot set and the time of generation also increase (see, Table 12 and Figure 15).

**Table 12.** The parameters used in Figure 15.

| Sr. No. | a | s | $\alpha$ | $\beta$ | $\gamma$ | $\delta$ | $\omega_1$ | $\omega_2$ | $\omega_3$ | $\omega_4$ | k |
|---|---|---|---|---|---|---|---|---|---|---|---|
| (a) | 0.4949 | 0.0909 | 0.0078 | 0.0056 | 0.0995 | 0.0312 | 0.8383 | 0.0119 | 0.7474 | 0.6556 | 2 |
| (b) | 0.4949 | 0.1515 | 0.0078 | 0.0056 | 0.0995 | 0.0312 | 0.8383 | 0.0119 | 0.7474 | 0.6556 | 2 |
| (c) | 0.4949 | 0.1919 | 0.0078 | 0.0056 | 0.0995 | 0.0312 | 0.8383 | 0.0119 | 0.7474 | 0.6556 | 2 |
| (d) | 0.4949 | 0.2323 | 0.0078 | 0.0056 | 0.0995 | 0.0312 | 0.8383 | 0.0119 | 0.7474 | 0.6556 | 2 |

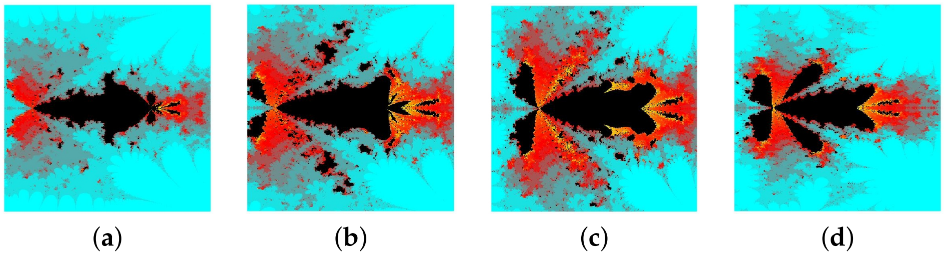


**Figure 15.** Effect of $s$ on Mandelbrot set in four-step iteration extended with s-convexity. (**a**) Area $[-0.8, 0.5] \times [-0.5, 0.5]$ and time 0.84 s. (**b**) Area $[-0.8, 0.5] \times [-0.8, 0.8]$ and time 0.88 s. (**c**) Area $[-1, 0.6] \times [-0.8, 0.8]$ and time 0.92 s. (**d**) Area $[-1, 1] \times [-1.5, 1.5]$ and time 0.92 s.

Changes in the shapes can be seen in the Figure 16a–d as the values of parameter $\alpha$ increase. The Mandelbrot set is rich in the colour black for larger values of $\alpha$ and is rich in the colour red for smaller values of $\alpha$ (see, Table 13 and Figure 16).

**Table 13.** The parameters used in Figure 16.

| Sr. No. | a | s | $\alpha$ | $\beta$ | $\gamma$ | $\delta$ | $\omega_1$ | $\omega_2$ | $\omega_3$ | $\omega_4$ | k |
|---|---|---|---|---|---|---|---|---|---|---|---|
| (a) | 0.4949 | 0.1919 | 0.0111 | 0.0056 | 0.0995 | 0.0312 | 0.8383 | 0.0119 | 0.7474 | 0.6556 | 2 |
| (b) | 0.4949 | 0.1919 | 0.1111 | 0.0056 | 0.0995 | 0.0312 | 0.8383 | 0.0119 | 0.7474 | 0.6556 | 2 |
| (c) | 0.4949 | 0.1919 | 0.6565 | 0.0056 | 0.0995 | 0.0312 | 0.8383 | 0.0119 | 0.7474 | 0.6556 | 2 |
| (d) | 0.4949 | 0.1919 | 0.9191 | 0.0056 | 0.0995 | 0.0312 | 0.8383 | 0.0119 | 0.7474 | 0.6556 | 2 |

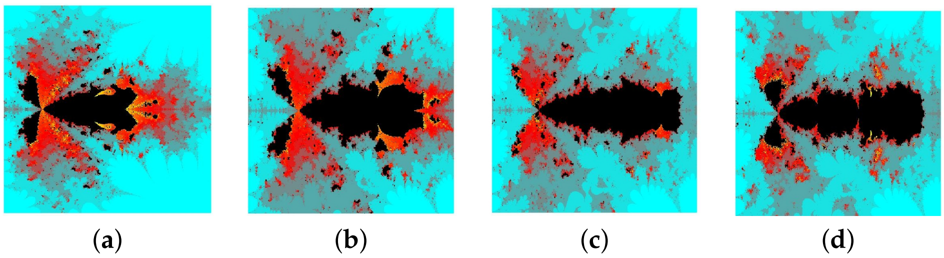


**Figure 16.** Effect of $\alpha$ on Mandelbrot set in four-step iteration extended with s-convexity. (**a**) Area $[-0.8, 0.5] \times [-0.5, 0.5]$ and time 0.82 s. (**b**) Area $[-0.9, 0.5] \times [-0.5, 0.5]$ and time 0.86 s. (**c**) Area $[-1, 0.6] \times [-0.5, 0.5]$ and time 0.89 s. (**d**) Area $[-1, 0.5] \times [-0.6, 0.6]$ and time 0.90 s.

As $\beta$ approaches 1, the black colour disappears. Higher values of $\beta$ add redness to the Mandelbrot set (see, Table 14 and Figure 17).

**Table 14.** The parameters used in Figure 17.

| Sr. No. | a | s | $\alpha$ | $\beta$ | $\gamma$ | $\delta$ | $\omega_1$ | $\omega_2$ | $\omega_3$ | $\omega_4$ | k |
|---|---|---|---|---|---|---|---|---|---|---|---|
| (a) | 0.4949 | 0.1919 | 0.0078 | 0.0000 | 0.0995 | 0.0312 | 0.8383 | 0.0119 | 0.7474 | 0.6556 | 2 |
| (b) | 0.4949 | 0.1919 | 0.0078 | 0.1234 | 0.0995 | 0.0312 | 0.8383 | 0.0119 | 0.7474 | 0.6556 | 2 |
| (c) | 0.4949 | 0.1919 | 0.0078 | 0.4567 | 0.0995 | 0.0312 | 0.8383 | 0.0119 | 0.7474 | 0.6556 | 2 |
| (d) | 0.4949 | 0.1919 | 0.0078 | 0.9999 | 0.0995 | 0.0312 | 0.8383 | 0.0119 | 0.7474 | 0.6556 | 2 |

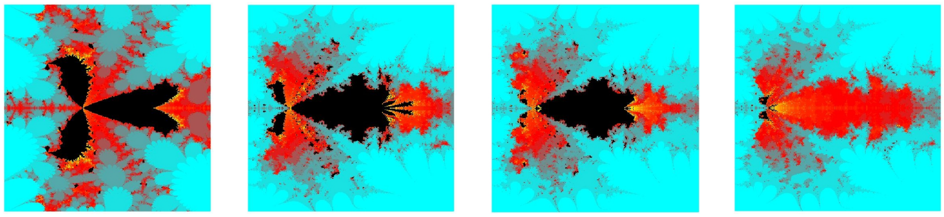

(**a**) (**b**) (**c**) (**d**)

**Figure 17.** Effect of $\beta$ on Mandelbrot set in four-step iteration extended with s-convexity. (**a**) Area $[-1.5, 1] \times [-1.5, 1.5]$ and time 0.82 s. (**b**) Area $[-1, 0.6] \times [-0.8, 0.8]$ and time 0.85 s. (**c**) Area $[-0.9, 0.5] \times [-0.5, 0.5]$ and time 0.88 s. (**d**) Area $[-0.8, 0.5] \times [-0.5, 0.5]$ and time 0.88 s.

Changes in the values of parameter $\gamma$ on the Mandelbrot set may be noticed in the following figures (see, Table 15 and Figure 18).

**Table 15.** The parameters used in Figure 18.

| Sr. No. | a | s | $\alpha$ | $\beta$ | $\gamma$ | $\delta$ | $\omega_1$ | $\omega_2$ | $\omega_3$ | $\omega_4$ | k |
|---|---|---|---|---|---|---|---|---|---|---|---|
| (a) | 0.4949 | 0.1919 | 0.0078 | 0.0056 | 0.0000 | 0.0312 | 0.8383 | 0.0119 | 0.7474 | 0.6556 | 2 |
| (b) | 0.4949 | 0.1919 | 0.0078 | 0.0056 | 0.000987 | 0.0312 | 0.8383 | 0.0119 | 0.7474 | 0.6556 | 2 |
| (c) | 0.4949 | 0.1919 | 0.0078 | 0.0056 | 0.0123 | 0.0312 | 0.8383 | 0.0119 | 0.7474 | 0.6556 | 2 |
| (d) | 0.4949 | 0.1919 | 0.0078 | 0.0056 | 0.64798 | 0.0312 | 0.8383 | 0.0119 | 0.7474 | 0.6556 | 2 |

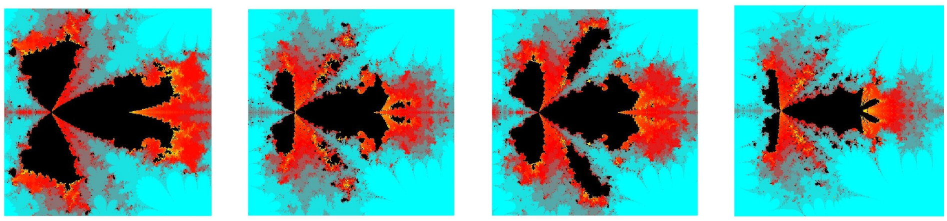

(**a**) (**b**) (**c**) (**d**)

**Figure 18.** Effect of $\gamma$ on Mandelbrot set in four-step iteration extended with s-convexity. (**a**) Area $[-1.5, 1] \times [-1.5, 1.5]$ and time 0.85 s. (**b**) Area $[-1, 0.6] \times [-0.8, 0.8]$ and time 0.87 s. (**c**) Area $[-0.9, 0.5] \times [-0.5, 0.5]$ and time 0.90 s. (**d**) Area $[-0.8, 0.5] \times [-0.5, 0.5]$ and time 0.92 s.

If the value of parameter $\delta$ increases, then the Mandelbrot set shrinks (see, Table 16 and Figure 19).

As we move from a four-step to a one-step iteration extended with s-convexity (as can be seen in Remark 2), the quintic Mandelbrot set becomes brighter, and takes less time to generate.

For $s = 1$ in Table 17, as we move from a four-step to a one-step iteration (as can be seen in Remark 2), we observe that the quintic Mandelbrot set in Figure 20a is entirely different while in Figure 20b–d, the shape is almost similar.

**Table 16.** The parameters used in Figure 19.

| Sr. No. | a | s | $\alpha$ | $\beta$ | $\gamma$ | $\delta$ | $\omega_1$ | $\omega_2$ | $\omega_3$ | $\omega_4$ | k |
|---|---|---|---|---|---|---|---|---|---|---|---|
| (a) | 0.4949 | 0.1919 | 0.0078 | 0.0056 | 0.0995 | 0.0009 | 0.8383 | 0.0119 | 0.7474 | 0.6556 | 2 |
| (b) | 0.4949 | 0.1919 | 0.0078 | 0.0056 | 0.0995 | 0.01234 | 0.8383 | 0.0119 | 0.7474 | 0.6556 | 2 |
| (c) | 0.4949 | 0.1919 | 0.0078 | 0.0056 | 0.0995 | 0.7356 | 0.8383 | 0.0119 | 0.7474 | 0.6556 | 2 |
| (d) | 0.4949 | 0.1919 | 0.0078 | 0.0056 | 0.0995 | 0.8387 | 0.8383 | 0.0119 | 0.7474 | 0.6556 | 2 |

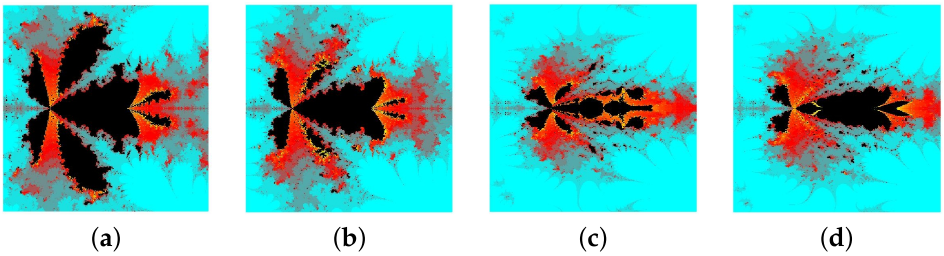

**Figure 19.** Effect of $\delta$ on Mandelbrot set in four-step iteration extended with s-convexity. (**a**) Area $[-1.5, 1] \times [-1.5, 1.5]$ and time 0.82 s. (**b**) Area $[-1, 0.6] \times [-0.8, 0.8]$ and time 0.87 s. (**c**) Area $[-0.9, 0.5] \times [-.5, 0.5]$ and time 0.91 s. (**d**) Area $[-0.8, 0.5] \times [-0.5, 0.5]$ and time 0.94 s.

**Table 17.** The parameters used in Figures 20–22.

| Sr. No. | a | s | $\alpha$ | $\beta$ | $\gamma$ | $\delta$ | $\omega_1$ | $\omega_2$ | $\omega_3$ | $\omega_4$ | k |
|---|---|---|---|---|---|---|---|---|---|---|---|
| (a) | 0.0568 | 0.5784 | 0.3599 | 0.5034 | 0.4089 | 0.5389 | 0.8383 | 0.0119 | 0.7474 | 0.6556 | 5 |
| (b) | 0.0568 | 0.5784 | 0.3599 | 0.5034 | 0.4089 | 0.0 | 0.8383 | 0.0119 | 0.7474 | - | 5 |
| (c) | 0.0568 | 0.5784 | 0.3599 | 0.5034 | 0.0 | 0.0 | 0.8383 | 0.0119 | - | - | 5 |
| (d) | 0.0568 | 0.5784 | 0.3599 | 0.0 | 0.0 | 0.0 | 0.8383 | - | - | - | 5 |

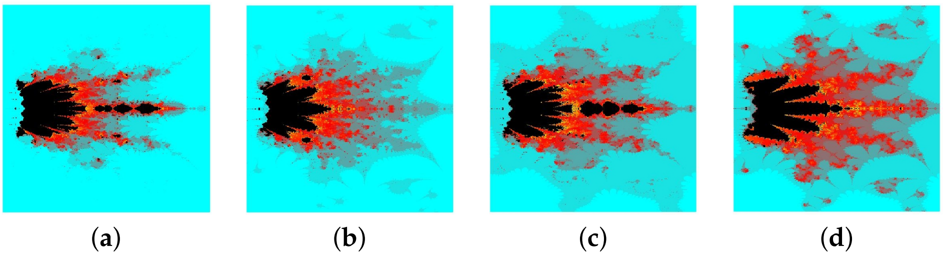

**Figure 20.** Effect of different iterations extended with s-convexity on Mandelbrot set. (**a**) Area $[-1.2, 0.7] \times [-1.5, 1.5]$ and time 1.16 s. (**b**) Area $[-1.2, 0.7] \times [-1.5, 1.5]$ and time 1.13 s. (**c**) Area $[-1.2, 0.7] \times [-1.5, 1.5]$ and time 1.11 s. (**d**) Area $[-1.2, 0.7] \times [-1.5, 1.5]$ and time 1.09 s.

One-step Picard iteration extended with s-convexity ($\alpha$ = 1 in Table 17; as can be seen in Figure 22a and Remark 2) adds beauty to the quintic Mandelbrot set. The shape is the improvement of the one obtained in a four-step iteration (see, Figure 21a). The shape of the Mandelbrot set remains the same, even for the standard Picard iteration ($s = 1$) (see, Figure 22).

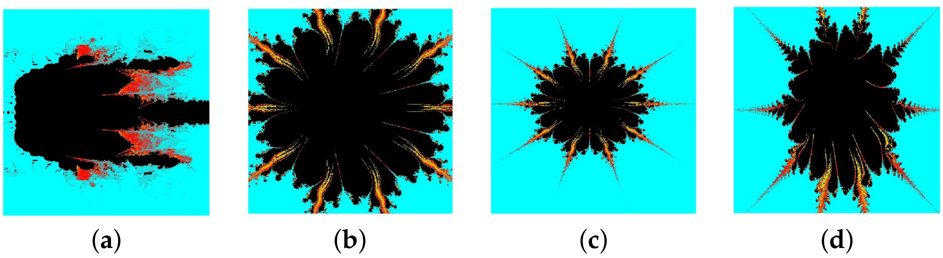

**Figure 21.** Effect of different standard four-step, Noor, Ishikawa, and Mann iteration on Mandelbrot set. (**a**) Area $[-1.2, 0.7] \times [-1.5, 1.5]$ and time 1.16 s. (**b**) Area $[-1.2, 0.7] \times [-1.5, 1.5]$ and time 1.13 s. (**c**) Area $[-1.2, 0.7] \times [-1.5, 1.5]$ and time 1.11 s. (**d**) Area $[-1.2, 0.7] \times [-1.5, 1.5]$ and time 1.09 s.

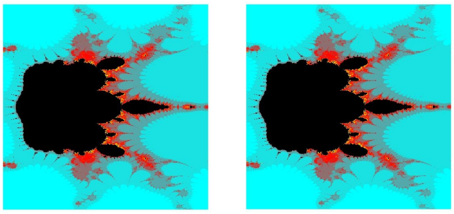

(**a**) (**b**)

**Figure 22.** Effect of Picard iteration extended with $s$-convexity and standard Picard iteration $(s = 1)$ on Mandelbrot set. (**a**) Area $[-1.2, 0.7] \times [-1.5, 1.5]$ and time 1.40 s. (**b**) Area $[-1.2, 0.7] \times [-1.5, 1.5]$ and time 1.48 s.

## 4. Conclusions

We extended the four-step fixed-point iteration with s-convexity to find escape radii and developed criteria for the complex-valued cosine functions. We investigated the mutants of Mandelbrot and Julia sets as fractals and observed that the dimensions of fractals using the four-step iteration extended with s-convexity relies on the convexity parameter s, and the parameters used in underlying iteration $\alpha, \beta, \gamma$, and $\delta$. We also observed that, for the real values of parameters $a$ and $c$, involved in the complex-valued cosine functions, fractals have symmetry with respect to the initial line, and for complex values, fractals become twisted. The examples show that the four-step iteration extended with s-convexity has the potential to generate new fascinating fractals. Our conclusions are more general and important from an application and a theoretical point of view for researchers of fixed-point theory, iterative methods, physics, textile engineering, etc. Furthermore, fractional mathematics is closely related to chaos and fractals. The fractional model in the Julia or Mandelbrot set always has local properties. Local fractional calculus has become a perfect tool for analyzing mathematical models and is a hot topic in mathematics. In the future, it is significant to study fractional mathematics from the perspective of fractals and applications (as can be seen in [39–41] etc.).

**Author Contributions:** Conceptualization, A.T., V.K. and M.S.; methodology, A.T. and V.K.; software, A.T., V.K. and M.S.; validation, A.T., V.K., U.S.R. and M.S.; formal analysis, A.T., V.K. and U.S.R.; investigation, A.T. and V.K.; writing—original draft preparation, A.T. and V.K.; writing—review and editing, M.S.; visualization, A.T., V.K., U.S.R. and M.S.; supervision, A.T. and U.S.R.; funding acquisition, M.S. All authors have read and agreed to the published version of the manuscript.

**Funding:** The researchers would like to thank the Deanship of Scientific Research, Qassim University, for funding the publication of this project.

**Data Availability Statement:** Not applicable.

**Acknowledgments:** Researcher would like to thank the Deanship of Scientific Research, Qassim University, for funding publication of this project.

**Conflicts of Interest:** The authors declare no conflict of interest.

## References

1. Abbas, M.; Nazir, T. A new faster iteration process applied to constrained minimization and feasibility problems. *Mat. Vesnik.* **2014**, *66*, 223–234.
2. Agarwal, R.P.; O'Regan, D.; Sahu, D.R. Iterative construction of fixed points of nearly asymptotically nonexpansive mappings. *J. Nonlinear Convex Anal.* **2007**, *8*, 61–79.
3. Alfuraidan, M.R.; Khamsi, M.A. Fibonacci–Mann iteration for monotone asymptotically nonexpansive mappings. *Bull. Aust. Math. Soc.* **2017**, *96*, 307–316. [CrossRef]
4. Berinde, V. Picard iteration converges faster than Mann iteration for a class of quasi-contractive operators. *Fixed Point Theory Appl.* **2004**, *2004*, 1–9. [CrossRef]
5. Ishikawa, S. Fixed points by a new iteration method. *Proc. Amer. Math. Soc.* **1974**, *44*, 147–150. [CrossRef]
6. Mann, W.R. Mean value methods in iteration. *Proc. Amer. Math. Soc.* **1953**, *4*, 506–510. [CrossRef]
7. Noor, M.A. New approximation schemes for general variational inequalities. *J. Math. Anal. Appl.* **2000**, *251*, 217–229. [CrossRef]

8. Picard, E. Memoire sur la theorie des equations aux derivees partielles et la methode des approximations successives. *J. Math. Pures Appl.* **1890**, *6*, 145–210.
9. Sintunavarat, W.; Pitea, A. On a new iteration scheme for numerical reckoning fixed points of Berinde mappings with convergence analysis. *J. Nonlinear Sci. Appl.* **2016**, *9*, 2553–2562. [CrossRef]
10. Barnsley, M. *Fractals Everywhere*, 2nd ed.; Academic Press: San Diego, CA, USA, 1993.
11. Brouers, F.; Sotolongo-Costa, O. Generalized fractal kinetics in complex systems (application to biophysics and biotechnology). *Phys. A Stat. Mech. Appl.* **2006**, *368*, 165–175. [CrossRef]
12. Hardy, H.H.; Beier, R.A. *Fractals in Reservoir Engineering*; World Scientific: Singapore, 1994.
13. Losa, G.A.; Nonnenmacher, T.F.; Merlini, D.; Weibel, E.R. *Fractals in Biology and Medicine*; Springer: Berlin/Heidelberg, Germany, 1994; Volume 3.
14. Thompson, A.H. Fractals in rock physics. *Annu. Rev. Earth. Planet. Sci.* **1991**, *19*, 237. [CrossRef]
15. Abbas, M.; Iqbal, H.; la Sen, M.D. Generation of Julia and Mandelbrot sets via fixed points. *Symmetry* **2020**, *12*, 86. [CrossRef]
16. Husain, A.; Nanda, M.N.; Chowdary, M.S.; Sajid, M. Fractals: An Eclectic Survey, Part-I. *Fractal Fract.* **2022**, *6*, 89. [CrossRef]
17. Kumar, D.; Sharma, J.R.; Jantschi, L. A novel family of efficient weighted-Newton multiple root iterations. *Symmetry* **2020**, *12*, 1494. [CrossRef]
18. Prajapati, D.J.; Rawat, S.; Tomar, A.; Dimri, R.C.; Sajid, M. A brief study of dynamics of Julia sets for entire transcendental function using Mann iterative scheme. *Fractals Fract.* **2022**, *6*, 397. [CrossRef]
19. Shahid, A.A.; Nazeer, W.; Gdawiec, K. The Picard–Mann iteration with s-convexity in the generation of Mandelbrot and Julia sets. *Monatsh. Math.* **2021**, *195*, 565–584.
20. Tanveer, M.; Kang, S.; Nazeer, W.; Kwun, Y. New tricorns and multicorns antifractals in Jungck Mann orbit. *Int. J. Pure Appl. Math.* **2016**, *111*, 287–302. [CrossRef]
21. Tomar, A.; Antal, S.; Prajapati, D.J.; Agarwal, P. Mandelbrot fractals using fixed-point technique of sine function. *Proc. Inst. Math. Mech. Natl. Acad. Sci. Azerb.* **2022**, *48*, 194–214. [CrossRef]
22. Antal, S.; Tomar, A.; Prajapati, D.J.; Sajid, M. Fractals as Julia sets of complex sine function via fixed point iterations. *Fractal Fract.* **2021**, *5*, 272. [CrossRef]
23. Ozgur, N.; Antal, S.; Tomar, A. Julia and Mandelbrot sets of transcendental function via Fibonacci-Mann iteration. *J. Funct. Spaces* **2022**, *13*, 2592573. [CrossRef]
24. Shatanawi, W.; Bataihah, A.; Tallafha, A. Four-step iteration scheme to approximate fixed point for weak contractions. *Comput. Mater. Contin.* **2020**, *64*, 1491–1504.
25. Julia, G. Mémoire sur l'itération des fonctions rationnelles. *J. Math. Pures Appl.* **1918**, *8*, 47–745.
26. Devaney, R.L. *A First Course in Chaotic Dynamical Systems, Theory and Experiment*, 2nd ed.; Addison-Wesley: Boston, MA, USA, 1992.
27. Mandelbrot, B.B. *The Fractal Geometry of Nature*; W. H. Freeman: New York, NY, USA, 1982.
28. Pinheiro, M. s-convexity, foundations for analysis. *Differ. Geom. Dyn. Syst.* **2008**, *10*, 257–262.
29. Cho, S.Y.; Shahid, A.A.; Nazeer, W.; Kang, S.M. Fixed point results for fractal generation in Noor orbit and s-convexity. *Springer Plus* **2016**, *5*, 1–16. [CrossRef]
30. Mishra, M.K.; Ojha, D.B.; Sharma, D. Fixed point results in tricorn and multicorns of Ishikawa iteration and s-convexity. *IJEST* **2011**, *2*, 157–160.
31. Nazeer, W.; Kang, S.; Tanveer, M.; Shahid, A. Fixed point results in the generation of Julia and Mandelbrot sets. *J. Inequal. Appl.* **2015**, *298*, 2015. [CrossRef]
32. Gdawiec, K. Fractal patterns from the dynamics of combined polynomial root finding methods. *Nonlinear Dyn.* **2017**, *90*, 2457–2479. [CrossRef]
33. Kang, S.M.; Rafiq, A.; Latif, A.; Shahid, A.A.; Kwun, Y.C. Tricorns and multicorns of-iteration scheme. *J. Funct. Spaces* **2015**, *2015*, 417167. [CrossRef]
34. Kumari, S.; Kumari, M.; Chugh, R. Dynamics of superior fractals via Jungck SP-orbit with s-convexity. *An. Univ. Craiova Math. Comput. Sci. Ser.* **2019**, *46*, 344–365.
35. Li, D.; Tanveer, M.; Nazeer, W.; Guo, X. Boundaries of filled Julia sets in generalized Jungck Mann orbit. *IEEE Access* **2019**, *7*, 76859–76867. [CrossRef]
36. Kwun, Y.C.; Shahid, A.A.; Nazeer, W.; Abbas, M.; Kang, S.M. Fractal generation via CR-iteration scheme with s-convexity. *IEEE Access* **2019**, *7*, 69986–69997. [CrossRef]
37. Antal, S.; Tomar, A.; Prajapati, D.J.; Sajid, M. Variants of Julia and Mandelbrot sets as fractals via Jungck-Ishikawa fixed point iteration system with s-convexity. *AIMS Math.* **2022**, *7*, 10939–10957. [CrossRef]
38. Tomar, A.; Antal, S.; Prajapati, D.J. Jungck-Noor fixed point iteration equipped with s convexity for visualizing Julia and Mandelbrot sets. *J. Funct. Spaces* **2023**, *in press*.
39. Dokuyucu, M.A. Caputo and atangana-baleanu-caputo fractional derivative applied to garden equation. *Turk. J. Sci.* **2020**, *5*, 1–7.

40. Dokuyucu, M.A. Analysis of the nutrient phytoplankton zooplankton system with non local and non singular kernel. *Turk. J. Inequal.* **2020**, *4*, 58–69.
41. İlknur, K.O.C.A.; Akcetin, E.; Yaprakdal, P. Numerical approximation for the spread of SIQR model with caputo fractional order derivative. *Turk. J. Sci.* **2020**, *5*, 124–139.